Research Article | Vol. 8, No. 7 | 1 Jul 2017 | BIOMEDICAL OPTICS EXPRESS 3395
Biomedical Optics EXPRESS

Flow-mediated dilatation test using optoacoustic imaging: a proof-of-concept

ANGELOS KARLAS,[1,2,3] JOSEFINE REBER,[1] GAEL DIOT,[2] DMITRY BOZHKO,[1] MARIA ANASTASOPOULOU,[1] TAREQ IBRAHIM,[3] MARKUS SCHWAIGER,[4] FABIEN HYAFIL,[4,5] AND VASILIS NTZIACHRISTOS[1,2,*]

[1]*HelmholtzZentrum München, Institute for Biological and Medical Imaging, 85764 Neuherberg, Germany*
[2]*Munich School of Bioengineering, Technische Universität München (TUM), 81675 Munich, Germany*
[3]*Klinikum rechts der Isar, Department of Cardiology, Ismaningerstrasse 22, 81675 Munich, Germany*
[4]*Klinikum rechts der Isar, Department of Nuclear Medicine, Ismaningerstrasse 22, 81675 Munich, Germany*
[5]*Bichat University Hospital, Department of Nuclear Medicine, Inserm 1148, University Diderot, Paris, France*
**v.ntziachristos@tum.de*

Abstract: Label-free multispectral optoacoustic tomography (MSOT) has recently shown superior performance in visualizing the morphology of human vasculature, especially of smaller vessels, compared to ultrasonography. Herein, we extend these observations towards MSOT interrogation of macrovascular endothelial function. We employed a real-time handheld MSOT scanner to assess flow-mediated dilatation (FMD), a technique used to characterize endothelial function. A data processing scheme was developed to quantify the dimensions and diameter changes of arteries in humans and determine wall distensibility parameters. By enabling high-resolution delineation of the blood-vessel wall in a cross-sectional fashion, the findings suggest MSOT as a capable alternative to ultrasonography for clinical FMD measurements.

OCIS codes: (110.5120) Photoacoustic imaging; (110.5125) Photoacoustics; (170.3880) Medical and biological imaging; (000.1430) Biology and medicine; (170.5380) Physiology.

References and links

1. R. G. Kolkman, J. H. Klaessens, E. Hondebrink, J. C. Hopman, F. F. de Mul, W. Steenbergen, J. M. Thijssen, and T. G. van Leeuwen, "Photoacoustic determination of blood vessel diameter," Phys. Med. Biol. **49**(20), 4745–4756 (2004).
2. A. Taruttis, A. C. Timmermans, P. C. Wouters, M. Kacprowicz, G. M. van Dam, and V. Ntziachristos, "Optoacoustic Imaging of Human Vasculature: Feasibility by Using a Handheld Probe," Radiology **281**(1), 256–263 (2016).
3. A. Dima and V. Ntziachristos, "Non-invasive carotid imaging using optoacoustic tomography," Opt. Express **20**(22), 25044–25057 (2012).
4. X. L. Deán-Ben and D. Razansky, "Functional optoacoustic human angiography with handheld video rate three dimensional scanner," Photoacoustics **1**(3-4), 68–73 (2013).
5. A. Dima, N. C. Burton, and V. Ntziachristos, "Multispectral optoacoustic tomography at 64, 128, and 256 channels," J. Biomed. Opt. **19**(3), 036021 (2014).
6. A. Taruttis and V. Ntziachristos, "Advances in real-time multispectral optoacoustic imaging and its applications," Nat. Photonics **9**(4), 219–227 (2015).
7. H. A. R. Hadi, C. S. Carr, and J. Al Suwaidi, "Endothelial dysfunction: cardiovascular risk factors, therapy, and outcome," Vasc. Health Risk Manag. **1**(3), 183–198 (2005).
8. M. A. Gimbrone, Jr., "Vascular endothelium: an integrator of pathophysiologic stimuli in atherosclerosis," Am. J. Cardiol. **75**(6), 67B–70B (1995).
9. M. C. Corretti, T. J. Anderson, E. J. Benjamin, D. Celermajer, F. Charbonneau, M. A. Creager, J. Deanfield, H. Drexler, M. Gerhard-Herman, D. Herrington, P. Vallance, J. Vita, and R. Vogel, "Guidelines for the ultrasound assessment of endothelial-dependent flow-mediated vasodilation of the brachial artery: a report of the International Brachial Artery Reactivity Task Force," J. Am. Coll. Cardiol. **39**(2), 257–265 (2002).
10. A. Rosenthal, V. Ntziachristos, and D. Razansky, "Acoustic Inversion in Optoacoustic Tomography: A Review," Curr. Med. Imaging Rev. **9**(4), 318–336 (2014).

#291379 https://doi.org/10.1364/BOE.8.003395
Journal © 2017 Received 24 Mar 2017; revised 30 Apr 2017; accepted 12 May 2017; published 23 Jun 2017

Biomedical Optics EXPRESS

11. N. Otsu, "A Threshold Selection Method from Gray-Level Histograms," IEEE Trans. Syst. Man Cybern. **9**(1), 62–66 (1979).
12. A. Fitzgibbon, M. Pilu, and R. Fisher, "Direct least square fitting of ellipses," IEEE Trans. Pattern Anal. Mach. Intell. **21**(5), 476–480 (1999).
13. M. F. O'Rourke, A. Pauca, and X. J. Jiang, "Pulse wave analysis," Br. J. Clin. Pharmacol. **51**(6), 507–522 (2001).
14. G. Baltgaile, "Arterial wall dynamics," Perspectives in Medicine **1**, 146–151 (2012).
15. M. R. Adams, J. Robinson, K. E. Sorensen, J. E. Deanfield, and D. S. Celermajer, "Normal ranges for brachial artery flow-mediated dilatation: A non-invasive ultrasound test of arterial endothelial function," J. Vasc. Invest. **2**(3), 146–150 (1996).
16. E. Dalli, L. Segarra, J. Ruvira, E. Esteban, A. Cabrera, R. Lliso, E. López, E. Llopis, and J. F. Sotillo, "[Brachial artery flow-mediated dilation in healthy men, men with risk factors, and men with acute myocardial infarction. Importance of occlusion-cuff position]," Rev. Esp. Cardiol. **55**(9), 928–935 (2002).
17. A. Peretz, D. F. Leotta, J. H. Sullivan, C. A. Trenga, F. N. Sands, M. R. Aulet, M. Paun, E. A. Gill, and J. D. Kaufman, "Flow mediated dilation of the brachial artery: an investigation of methods requiring further standardization," BMC Cardiovasc. Disord. **7**(1), 11 (2007).
18. F. U. Mattace-Raso, T. J. van der Cammen, A. Hofman, N. M. van Popele, M. L. Bos, M. A. Schalekamp, R. Asmar, R. S. Reneman, A. P. Hoeks, M. M. Breteler, and J. C. Witteman, "Arterial stiffness and risk of coronary heart disease and stroke: the Rotterdam Study," Circulation **113**(5), 657–663 (2006).
19. F. A. Chaudhry, S. Bangalore, S. Upadya, A. Shah, H. Eftekhari, D. Pudpud, and C. M. Sehgal, "Cross-sectional imaging identifies flow-mediated vasodilatation more accurately compared with longitudinal imaging," J. Am. Soc. Echocardiogr. **20**(12), 1380–1385 (2007).
20. M. Charakida, E. de Groot, S. P. Loukogeorgakis, T. Khan, T. Lüscher, J. J. Kastelein, T. Gasser, and J. E. Deanfield, "Variability and reproducibility of flow-mediated dilatation in a multicentre clinical trial," Eur. Heart J. **34**(45), 3501–3507 (2013).
21. A. Y. Nasr, "The radial artery and its variations: anatomical study and clinical implications," Folia Morphol. (Warsz) **71**(4), 252–262 (2012).
22. A. B. Karpiouk, B. Wang, and S. Y. Emelianov, "Development of a catheter for combined intravascular ultrasound and photoacoustic imaging," Rev. Sci. Instrum. **81**(1), 014901 (2010).
23. B. Wang, A. Karpiouk, D. Yeager, J. Amirian, S. Litovsky, R. Smalling, and S. Emelianov, "In vivo intravascular ultrasound-guided photoacoustic imaging of lipid in plaques using an animal model of atherosclerosis," Ultrasound Med. Biol. **38**(12), 2098–2103 (2012).
24. C. Vinegoni, I. Botnaru, E. Aikawa, M. A. Calfon, Y. Iwamoto, E. J. Folco, V. Ntziachristos, R. Weissleder, P. Libby, and F. A. Jaffer, "Indocyanine green enables near-infrared fluorescence imaging of lipid-rich, inflamed atherosclerotic plaques," Sci. Transl. Med. **3**(84), 84ra45 (2011).
25. A. L. Huang and J. A. Vita, "Effects of systemic inflammation on endothelium-dependent vasodilation," Trends Cardiovasc. Med. **16**(1), 15–20 (2006).

1. Introduction

Optoacoustic contrast in the near-infrared region (650-850 nm) is attributed primarily to light absorption by oxygenated and deoxygenated hemoglobin. Since blood vessels concentrate high amounts of hemoglobin, they present excellent targets for optoacoustic imaging [1]. Recently, the capacity of optoacoustic tomography to visualize human vasculature was compared with ultrasound and Doppler ultrasound [2]. It was shown that the optoacoustic method outperforms ultrasonography, by providing a more accurate vessel representation, in particular regarding meso- and micro-vasculature. Overall, the multispectral optoacoustic tomography (MSOT) ability to resolve human vasculature has been demonstrated in several reports, using different scanner configurations [3,4]. We have shown that image quality significantly improves when using curved ultrasound detectors, over linear detectors [5]. Moreover, recent development of fast-tuning lasers offering >50 mJ energy per pulse has allowed the application of single-pulse-per-frame (SPPF) acquisition [6], which uses a single laser pulse to collect a cross-sectional image from tissue without averaging data from multiple pulses. SPPF minimizes motion artifacts and allows image collection at >50 Hz frame rates. Nevertheless, the potential of SPPF for MSOT interrogation of physiological processes and vascular dynamics remains largely unexplored.

In this work we employed SPPF optoacoustic tomography using curved array detectors to characterize its utility in flow-mediated dilatation (FMD) tests. FMD, typically performed using ultrasound (US), measures the increase in the diameter of a peripheral artery in response to a temporary (usually 5 min) blood flow occlusion. These changes provide an

Biomedical Optics EXPRESS

indication of the functional status of the vascular endothelium, which is thought to influence risk of cardiovascular disease [7] and relate to atherosclerosis [8]. FMD measurements were carried out by a cardiology specialist on healthy, non-smoking Caucasian volunteers. Procedures were conducted in accordance with published guidelines on ultrasound-based endothelial-dependent FMD measurement of the brachial artery [9].

2. Methods

2.1 MSOT system and image acquisition

MSOT data were collected with a custom-built handheld system at 50 Hz frame rate [3]. A diode-pumped solid state Nd:YAG tunable laser (Spitlight DPSS OPO, Innolas Laser GmbH, Germany) was used for illumination between 700 nm and 960 nm using 8 ns pulse duration and 17 mJ energy per pulse (at 700 nm, highest-energy wavelength). Light was delivered to tissue through a fiber bundle (CeramOptec GmbH, Germany), attached next to a 256 piezoelectric elements detector with 5 MHz central frequency. The detector elements were arranged in a curved configuration with a radius of 60 mm, providing 174-degree coverage (Imasonic SAS, France). A sealed, flexible plastic membrane was placed around the detector and enclosed with water for coupling ultrasound waves from the tissue to the detector. Analog signals were sampled, amplified and recorded in parallel, using a 256-channel data acquisition card (DAQ) with 12-bit precision in each channel. High resolution (100 μm) of 60 × 60 mm (600 × 600 pixels) images were produced by a back-projection reconstruction method [10] using the ViewMSOT reconstruction software (Xvue Ltd, Greece). US data were acquired with a commercial system (Logiq E9, GE, USA) equipped with a linear matrix array transducer (ML6-15), which is usually used for vascular applications, operating at a frequency of 12MHz.

Healthy volunteers (n = 4, Subject #1: M-32, Subject #2: F-33, Subject #3: M-32, Subject #4: M-27) consumed no food, caffeine or medication for at least 10 h before the experiment, which was performed in a quiet, dark room at room temperature. They were positioned supine and the radial artery could be easily identified due to its characteristic shape and wall motion during the cardiac cycle by both US and MSOT imaging. The radial artery was imaged 5 cm proximal to the wrist joint using MSOT and 3 cm more proximally using US to avoid ultrasonic signal interference between the two hand-held probes during simultaneous imaging which significantly decreased the MSOT image quality. The artery was imaged along the transverse plane with both imaging modalities. All FMD tests were carried out according to guidelines for the ultrasound assessment of FMD of the brachial artery [9] by scanning the forearm region over the radial artery for 2 min at rest, 5 min during cuff application (cuff-on period: total occlusion induced by a cuff pressure equal to the systolic blood pressure increased by 50 mmHg), and 2 min after the release of blood flow, with an MSOT frame rate of 50 Hz. For the US measurements ink skin markings ensured the consistent localization of the same arterial cross-section before and 60 sec after the cuff-on period.

Multiple pilot measurements were performed over the forearm region of each volunteer to obtain baseline measurements and FMD readouts. At first, cross-sectional MSOT images of the forearm were obtained at different wavelengths over the (700 nm - 900 nm) spectral range clearly depicting the radial artery and several neighboring vessels due to their high hemoglobin concentration and light absorption signal. Illumination wavelength at ~800 nm was found to offer the best contrast, over other wavelengths. To increase temporal resolution and enable accurate tracking of the arterial wall dimensions over the whole scanning period (Fig. 1(a)), we selected 800 nm for dynamic measurements during the cuff application. This wavelength represents the isosbestic point in the hemoglobin absorption spectrum and therefore the images are not affected by changes in the content of oxy- and deoxygenated hemoglobin in blood vessels. The radial artery was in lateral contact with a set of parallel vessels (adjacent vessels) creating a complex vascular structure with characteristic cross-sectional shape (Fig. 1(a), Fig. 1(b)).

Biomedical Optics EXPRESS

2.2 Artery segmentation and diameter tracking

To accurately determine the diameter changes of the radial artery, required by the FMD test, we performed an artery segmentation procedure, consisting of several steps. Accurate segmentation required correction of the optoacoustic signal variation across the lumen cross-section due to depth-dependent light attenuation. The vascular complex was interactively identified by the user on the first frame of the acquired image series, and this location was registered for all subsequent images acquired (Fig. 1(a), Fig. 1(b)). All images were then converted to binary by applying a threshold based on the Otsu's global image thresholding method [11]. White pixels not connected to the vascular complex of interest were considered as noise and eliminated. The vascular complex was then fitted to an ellipse (circumscribing) and attenuation correction was applied along the short axis of the ellipse, for all areas in the original image that were above the threshold. Although photon attenuation follows an exponential decay, a linear correction sufficed herein to sufficiently smooth the signal distribution in the radial artery (Fig. 1(c)). Following attenuation correction, a second threshold was applied using Otsu's method [11] and the resulting binary silhouette of the entire radial complex was smoothed via morphological operations and the convex hull of the radial artery was finally revealed (Fig. 1(d)). To track the diameter changes of the radial artery over time, the Fitzgibbon's direct least-squares method [12] was applied to fit an ellipse onto the edge of the binary silhouette (Fig. 1(e)). Fluctuations in the minor and major axes of the fitted ellipses were calculated over the entire FMD recording period for Subject #1 (Fig. 2(a), Fig. 2(b)) and used to extract information about the FMD response and functional parameters of the arterial wall (e.g. wall strain, cross sectional distensibility) for every cardiac cycle. The same algorithm was applied on selected frames of the MSOT recordings before and at 60 sec after the cuff-on period for all subjects to extract the FMD responses. Furthermore, the minor and major cross-sectional axes of the radial artery were measured manually by a cardiology specialist on both MSOT and US data at rest and 60 sec after the end of occlusion providing the potential to assess the performance of MSOT in comparison to the gold-standard traditional US imaging under the same conditions when imaging peripheral arteries in humans *in vivo* (Fig. 3(a)).

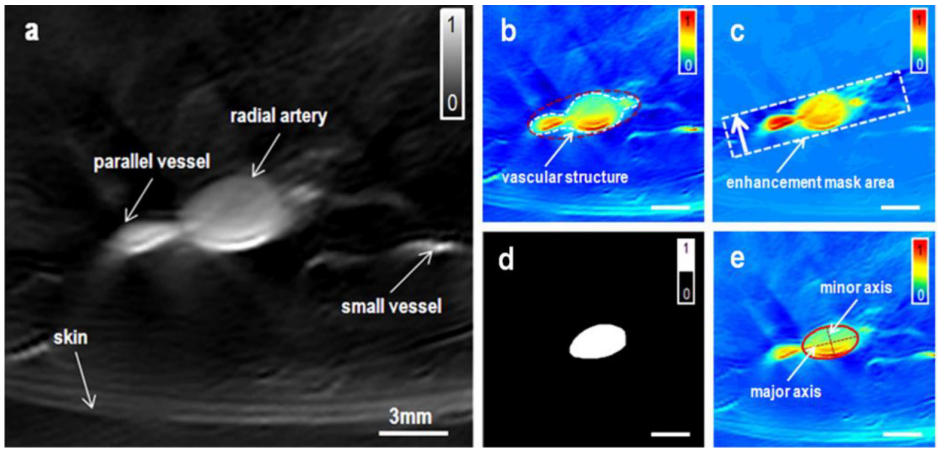

Fig. 1. Multispectral optoacoustic tomography (MSOT) imaging of the radial artery in the forearm region (Subject #1). (a) Gray-scale optoacoustic image of the radial artery and neighboring vessels obtained at 800nm prior to occlusion. (b) Same image as in (a) using a different color map with the white dashed line indicating the vascular structure of interest and the red dashed line indicating the circumscribing ellipse. (c) Result of attenuation correction step after applying the enhancement mask on the area marked with the white dashed line. The thick white arrow in the marked area indicates the direction of linear signal amplification. (d) Segmented lumen of the radial artery. (e) Final fitted ellipse with its major and minor axis representing the radial artery. All scale bars are 3mm.

Biomedical Optics EXPRESS

2.3 Calculation of arterial distensibility and FMD response

By plotting the lengths of the minor axes of the fitted ellipses over the whole recording period of the optoacoustic measurement corresponding to Subject #1, we observed that they follow a periodic pattern identical to the expected recording of the radial blood pressure wave over a cardiac cycle [13] (Fig. 2(c), Fig. 2(d)). We employed the periodic pattern of the lengths of the ellipses minor axes to identify the time points corresponding to the cardiac systole and diastole. Thus, we recorded the peak of the minor axis of the ellipse as a function of time, to identify the maxima and minima for each cardiac cycle. Based on the known physiological radial blood pressure fluctuations over a cardiac cycle [13], an intuitive assumption has been made that each highest peak corresponded to the peak-systolic point in the cardiac cycle, while the next lowest peak corresponded to the end-diastolic point of the same cycle. The fluctuations in the minor axis of the ellipse during each cardiac cycle determine the per-cycle diameter-based distensibility or wall strain (WS) of the artery over the periods before and after total occlusion (Eq. (1) [14]):

$$WS = \frac{Ds - Dd}{Dd} \tag{1}$$

where Ds refers to systolic minor axis of the ellipse and Dd to diastolic minor axis. The cross-sectional distensibility (CD) was calculated based on the cross-sectional area as follows (Eq. (2) [14]):

$$CD = \frac{As - Ad}{Ad} \tag{2}$$

where As refers to systolic cross-sectional area of the ellipse and Ad to diastolic cross-sectional area. The ellipse cross-sectional area (EA) was calculated as (Eq. (3)):

$$EA = \frac{\pi\alpha\beta}{4} \tag{3}$$

where α is the major axis length and β is minor axis length evaluated empirically. We then interrogated whether FMD responses can be calculated by observing the radial artery diameter, considering the diameter as either the minor or the major axis of the fitted ellipse. FMD calculations were related to the radial artery diameter as:

$$FMD = \frac{HD - BD}{BD} \times 100\% \tag{4}$$

where HD refers to the hyperemia diameter of the artery, defined as the diameter at 60 seconds after the end of occlusion, while BD refers to the baseline diameter of the measured artery at rest. The same formula was used to calculate the FMD responses for all subsequent MSOT measurements of all subjects.

3. Results

First, we tracked the calculated minor and major axes of the radial artery over the whole MSOT recording period. Figure 2(a) and Fig. 2(b) depict fluctuations in the diameter of the ellipse for Subject #1 over 70 seconds prior and after occlusion respectively. As expected, the lengths of both the minor and major axes of the fitted ellipse progressively decrease after the inflation of the cuff above the systolic blood pressure indicating the gradual closing of the artery. The radial artery needed about 50 seconds to close completely and become invisible on MSOT. The lengths of the two axes increase acutely after cuff deflation, indicating the acute opening of the radial artery in response to the full release of blood flow. As can be seen, changes in the minor and major axes show different temporal patterns. Figure 2(c) and Fig.

Biomedical Optics EXPRESS

2(d) indicate that the fluctuations of minor axis reflect more closely the physiological changes in arterial blood pressure during one cardiac cycle, enabling differentiation between the systolic and diastolic phases. In contrast, the pattern of fluctuations in major axis length, showed less variation within each cycle but greater variation across longer periods of time, as for example over the following two time periods: seconds #45-55 before occlusion (Fig. 2(a)) and seconds #10-20 seconds after occlusion (Fig. 2(b)).

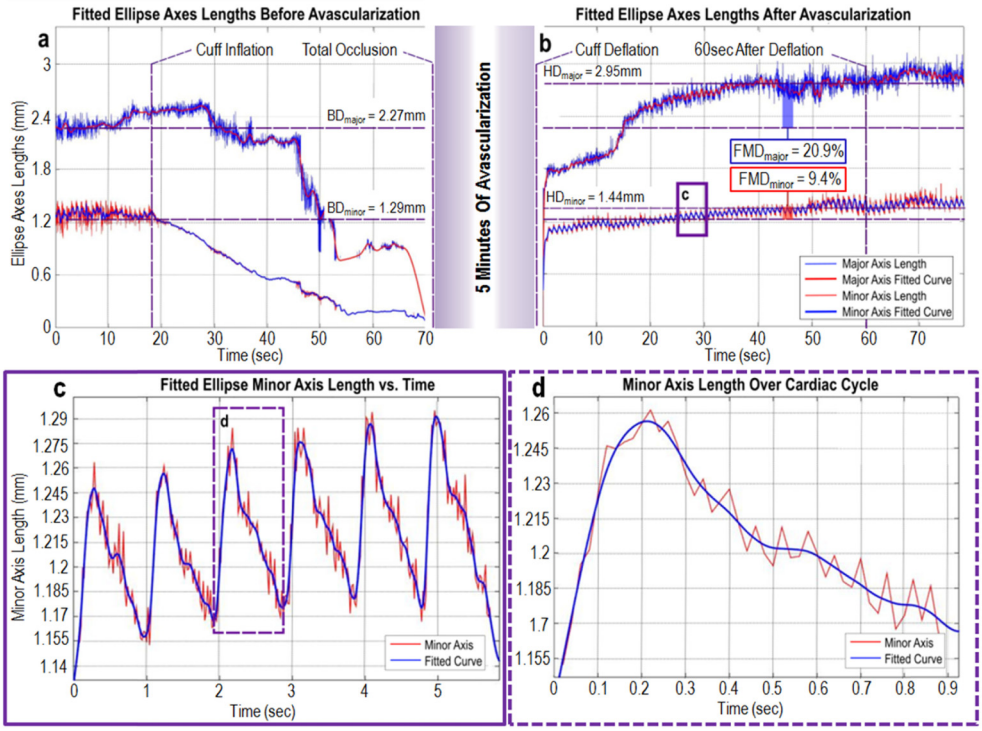

Fig. 2. Multispectral optoacoustic tomography (MSOT)-derived readouts of the minor and major axes of the fitted ellipse over the flow-mediated dilatation (FMD) measurement. (a) Axes fluctuations before complete arterial occlusion. (b) Axes fluctuations after a 5-min avascularization (total occlusion) period. (c) Minor axis changes over a 6-second period after release of arterial occlusion. Expanded from the boxed area in (b). (d) Fluctuations of the minor axis length during a cardiac cycle after arterial occlusion marked also in (c).

Next, we determined the per-cycle diameter-based distensibility or wall strain (WS) of the radial artery wall, based on Eq. (1). We also calculated the cross-sectional distensibility (CD) based on fluctuations in best-fitting ellipse area for the same subject (Eq. (2), Eq. (3)). Figure 3(a) and Fig. 3(b) depict the beat-to-beat arterial distensibility for Subject #1, during two 12-second periods before and after occlusion, respectively (seconds #1-12 before complete arterial occlusion occurs and seconds #54-66 after the end of complete occlusion). As can be seen, the distensibility differed before and after the end of total occlusion. It is also of interest that the distensibility at either of these time periods differed depending on whether the minor axis or ellipse area was used in the calculation.

Finally, FMD responses of all volunteers were calculated by extracting the hyperemia diameter and the baseline diameter for each axis of the fitted ellipse (HD_{minor}/HD_{major} and BD_{minor}/BD_{major}) to estimate the FMD response corresponding to each axis according to Eq. (4). For example, based on absolute minor axis measurements, the baseline diameter BD_{minor} for Subject #1 was 1.29 mm and HD_{minor} = 1.44 mm, corresponding to FMD_{minor} of 9.4%. A much higher FMD_{major} of 20.9% was obtained using the extracted major axis values (BD_{major} =

Biomedical Optics EXPRESS

2.27 mm, HD_{major} = 2.95 mm). Nevertheless, both FMD calculations fell within the normal range reported in various studies, which may vary by as much 20% in the case of the brachial artery [15–17]. Figure 3c shows the FMD responses for the minor and major axes of the radial artery for all subjects as represented by the corresponding ellipse axes. The mean ± standard deviation of the FMD_{minor} was 11.4 ± 3.3% and of the FMD_{major} was 26.1 ± 6.4%.

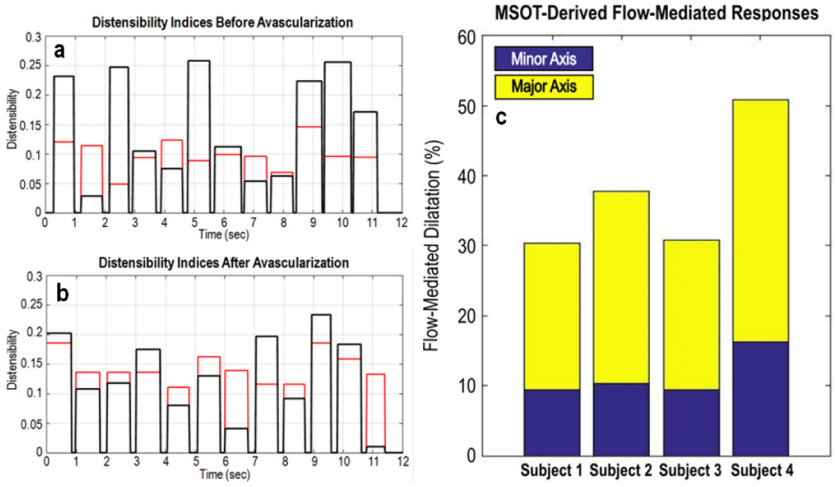

Fig. 3. MSOT-derived distensibility parameters of the radial artery and FMD responses. Beat-to-beat arterial distensibility before (a) and after (b) occlusion, respectively for Subject #1. Black bars: estimated area-based cross-sectional distensibility (CD), Red bars: diameter-based distensibility or wall strain (WS). (c) MSOT-derived FMD responses for all subjects (n = 4).

As a last step, we compared the MSOT and US accuracy to track arterial dimensions. A cardiology specialist measured the minor and major axes of the radial artery cross-section at rest and at 60 seconds after the end of cuff-occlusion on characteristic selected frames of both MSOT and US recordings for 3 subjects (Subject #2-4) (Fig. 4(a), Fig. 4(b)). The specialist measured each axis 3 times on every frame provided. The mean value of the 3 measurements was tabulated as the axis length. Figure 4c depicts the absolute values of the manually measured minor and major axes of the cross-section of all radial arteries as extracted from MSOT and US data at two different time points: before occlusion and 60 sec after the end of arterial occlusion. By using US, the minor arterial axis was calculated to be 1.97 ± 0.16 mm and the major axis 2.62 ± 0.31 mm across the cohort of subjects #2, 3 and 4. By employing MSOT the minor axis was estimated to be 2.02 ± 0.22 mm and the major cross-sectional axis 2.51 ± 0.29 mm. To provide a metric of the intraobserver error, as well as the error introduced by the image quality, the cardiology specialist conducted 10 subsequent manual measurements of both the minor and major axes of the arterial cross-section in two high-quality random MSOT and US frames. The mean ± standard deviation values were estimated to be 1.85 ± 0.07 mm for the minor axis and 2.51 ± 0.07 mm for the major axis using US. The MSOT-derived corresponding values were: 2.47 ± 0.04 mm for the minor axis and 3.46 ± 0.05 mm for the major cross-sectional axis.

Biomedical Optics EXPRESS

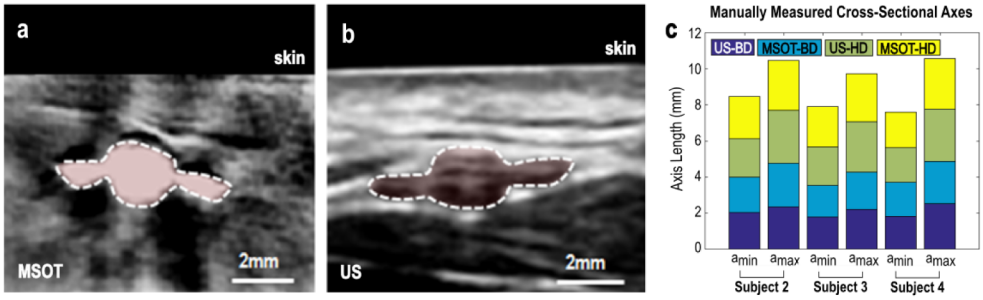

Fig. 4. Comparison between MSOT and US imaging of the radial artery. (a) Characteristic MSOT frame of the radial artery cross-section of Subject #4 at rest. (b) Characteristic US frame of the radial artery cross-section of Subject #4 at rest. The dashed lines delineate the vascular complex of interest in both images. (c) Manually measured cross-sectional arterial axes lengths for Subjects #2-4 extracted from US and MSOT images before and 60 sec after occlusion. BD: Baseline Diameter, HD: Hyperemia Diameter.

4. Discussion and conclusion

This study presents a proof of concept for the use of MSOT for real-time FMD testing of macrovascular endothelial function in humans within the clinical setting. It takes advantage of a recently developed hand-held device and a customized computational method, to image the radial artery and track changes in its diameter with high temporal resolution. MSOT FMD tests relied on imaging the radial artery cross-section and quantitatively assessing its contour using a fitted ellipse. Additional information was also obtained about arterial wall distensibility whose decrease (or else increase in wall stiffness) has been associated with raised risk of cardiovascular disease [18].

The herein described approach presents a novel and very promising tool for FMD testing which may be considered as an alternative to ultrasonography, since it offers much better vessel wall contrast and resolution compared to ultrasound images that are affected by speckle. Furthermore, MSOT demonstrates clinically acceptable accuracy compared to US with regards to the capability of tracking arterial wall dimensions (Fig. 4c). Ultrasound imaging usually resolves vessels along the longitudinal dimension as it offers poor vessel wall delineation in cross-sectional images [9]. Then, FMD tests are performed by recording the arterial diameter as it is calculated based on the central longitudinal plane of the artery visualized. Compared to adjacent planes, fluctuations in the central plane of the vessel (along the longitudinal dimension) are the highest, optimizing the sensitivity in detecting vessel wall fluctuations over time. Nevertheless, accurate FMD measurements based on ultrasound imaging are challenging since they require identification of the central plane and a long-term fixation of the ultrasound probe over the long arterial axis, which can lead to errors due to motion. Conversely, transversal (cross-sectional) scanning of vessels overcome the limitations of ultrasound imaging and possibly offers greater flexibility and accuracy for precise tracking of the vessel diameters across the cross-section [19].

Nevertheless, larger cohorts and more systematic studies are needed for a detailed comparison between MSOT and US imaging not only regarding the tracking of arterial dimensions in humans but also the extraction of FMD readouts. A series of error sources challenges the reliability of such a comparison. The artery under investigation should be imaged at exactly the same position with both the MSOT and US probes during the same recording, to avoid the intrasession, intraobserver, and intrasubject variability of FMD responses [20]. This could be achieved by a new generation of hybrid MSOT/US systems using a common transducer. Furthermore, the radial artery is characterized by variable diameter across its length which further influences the calculated values [21]. The development of accurate automated methods for arterial segmentation in both MSOT and US

Biomedical Optics EXPRESS

images is of great importance since the manual segmentation of the arterial silhouette is not only time-consuming but it may also introduce inaccuracies that further degrade the result.

As presented, we further observed differences in the post-occlusion dilatatory responses between recordings of the minor and major cross-sectional arterial axes from Subject #1. Indeed, contrary to the major axis, which showed a diphasic increase after the end of occlusion (first increase at second #0 and second additional increase around second #15 post-occlusive; Fig. 1(b)), the response of the minor axis was monophasic and quickly stabilized at an average length, while showing fine fluctuations over the cardiac cycle. These findings show considerable axis- and plane-related variability of FMD response, which may help explain the wide range of normal FMD values in the literature [15–17]. Our findings also highlight the need for greater standardization of FMD tests, and demonstrate the advantage of using a cross-sectional analysis.

Fluence correction was found necessary for improving the performance of lumen segmentation and accurate wall delineation. With the proposed method we detected radial artery diameters as small as 0.17 mm (based on the minor axis; Fig. 2(a)), which is close to the resolution limit of 100 μm of the MSOT system employed. Improvements in the segmentation and tracking processes may enable monitoring of even smaller vascular structures, potentially using a fully automated framework. The herein combination of precise ellipse fitting and 50 Hz temporal resolution further allowed observation of arterial wall dynamics, which have been identified as an independent risk factor for premature cardiovascular disease [14].

Future steps of MSOT-based cardiovascular applications may make use of lipid readings for identifying atherosclerotic lesions [6,22,23], while the use of indocyanine green (ICG) might empower molecular studies of plaque inflammation [24]. With arrival of improved chromophores, MSOT could enable the interrogation of a wider range of processes and functions offering pathophysiological readings of disease that may affect the FMD response [25]. The results of the current study testified the possible utility of MSOT over ultrasonography for FMD measurements. An extensive study of FMD responses on healthy volunteers and patients may lead to a precise comparison of MSOT and US and encourage future research into the assessment of arterial wall dynamics and vascular biology.

Funding

Deutsche Forschungsgemeinschaft (DFG) of Germany (CRC 1123 (Z1); NT 3/10-1); Research Council (ERC) under the European Union's Horizon 2020(694968 (PREMSOT)).

Acknowledgments

We thank Prof. Dr. C. Weber, Prof. Dr. M. Hrabě de Angelis, Dr. A. Bühler, Dr. S. Ovsepian, and Dr. A. C. Rodriguez for the valuable support and discussions.